Response to community comment

CC1: 'Comment on egusphere-2025-3596', Ousmane O. Sy

Thank you very much for carefully reading the manuscript and for providing such thoughtful and insightful comments. Based on your feedback, I have revised the manuscript to improve its clarity and to incorporate the changes in the revised submission. My point-by-point responses are provided below in red. Please note that the line numbers indicated in our responses refer to a revised version of the manuscript.

This article presents very interesting results based on a triple-frequency dataset complemented by Doppler measurements of the ESA/JAXA EarthCARE mission. It shows the high potential of coincident multi-frequency remote sensing observations with reflectivity, Doppler and passive microwave measurements. Such superdatabase can definitely help studies of dynamic atmospheric processes. The thermal analysis of the Doppler measurements is also eye-opening.

Thank you for recognizing the importance of our study. We plan to make the dataset, including passive microwave observations by GMI radiometer, publicly available from the JAXA server in the near future, and we hope that these data will contribute to a wide range of future analyses in atmospheric science.

My minor comments are detailed below.

Comments:

1. Equation 1: Given the convention to represent updrafts as positive velocities, I think the equation should be

In this study, positive values of Doppler velocity (V_d) are defined as upward motion. Likewise, we define the vertical upward direction as positive for both V_t and $V_{\rm air}$, so the fall velocity V_t is always negative, as shown in Eq. (5) and Eq. (7). Therefore, we believe that the formulation in Eq. (1) is correct as it stands. In the CPR L2a cloud product (CPR_CLP), terminal fall velocity is also defined as negative, and to ensure consistency with that product, we would like to maintain this definition. We have added the following explanation regarding the negative sign of V_t :

Line 194

In this paper, positive values of V_d are defined as upward direction. Therefore, positive V_{air} means upward air motion and V_t is always negative.

2. Equation 2: the denominator is directly proportional to the reflectivity factor, but there is the factor (¥lambda^4/¥pi^5|K_W|^2) missing, unless it is implicit in the definition of ¥sigma_b?

As the reviewer correctly pointed out, a factor of $\lambda^4/\pi^5|K_w|^2$ must be applied when calculating the reflectivity

factor. We have added the explanation, as shown below:

Line 198

The denominator of Eq. (2), when multiplied by $\lambda^4/\pi^5|K_w|^2$, where λ is the radar wavelength and K_w is the normalizing dielectric factor, corresponds to the radar reflectivity factor (Z).

3. Equation 1 represents all the error terms as additive (¥epsilon), which is a simplification. In fact there is also a multiplicative factor (which includes the randomness of the signal) that can be mitigated only by adaptive filtering, or along-track integration. Could you please include this caveat?

Thank you for this important comment regarding Doppler errors. As you pointed out, the term ε includes not only systematic biases but also random uncertainties arising from measurement noise. We have added the following caveat:

Line 203-205

In Eq. (2), ε is expressed as an additive term, but it includes not only systematic biases, but also random uncertainties mentioned above that can only be mitigated by adaptive filtering or along-track integration.

4. Line 211: It is true that the Doppler velocity comes from the phase change of the lag-1 correlation function, which in turns is not affected by attenuation. However, the magnitude of this correlation function (module of a complex number) is important to have reliable Doppler. Otherwise, the Doppler is all salt-and-pepper.

Thank you again for this important comment. We agree that, under conditions of strong attenuation or multiple scattering, the correlation may decrease to the point where Doppler information can no longer be retrieved. We believe that such cases are largely excluded by applying the multiple scattering filtering criteria of Battaglia et al. (2011), and therefore the impact on the statistics shown in Section 3 is expected to be small. However, we acknowledge that the original wording could cause misunderstanding, so we have revised it as follows:

Line 222-229

In contrast, V_d is retrieved from the pulse-to-pulse phase difference rather than from signal amplitude (Eisinger et al. 2024), and is therefore intrinsically less affected by attenuation of returned power (Doviak and Zrnic, 1993). In practice, pulse-to-pulse phase correlation is maintained under moderate attenuation, allowing the velocity retrievals to remain stable (Tian et al., 2007; Kollias et al., 2014). The main limitation arises when severe attenuation and multiple scattering associated with heavy rain or ice precipitation substantially degrades the pulse-to-pulse phase correlation, leading to large errors (Matrosov, 2008; Battaglia et al., 2011). In this study, cases containing rain, wet snow, and graupel were retained, while severe attenuation were excluded by applying screening following Battaglia et al. (2011), leading to preserve physically meaningful velocity information in these hydrometeor regimes.

5. Line 225: Does the use of Mie mean that it does not account for the shape/density variation of the frozen hydrometeors and their non-sphericity? Is that considered negligible microphysical variation?

For frozen hydrometeors, we assume homogeneous spherical particles with a fixed density. As you pointed out, it is indeed important to consider the shape and density variations of ice particles when evaluating

backscattering and terminal fall velocities. Significant differences are expected among snow, graupel, and hail. However, CPR observations, which are limited to the nadir direction, inherently provide no information to constrain the spherical assumption used here. This contrasts with ground-based dual-polarization radars, which observe the hydrometeor from the side, where particle asymmetry is more evident and can provide additional information. In this study, we therefore focus on rainfall V_t , where the spherical assumption is reasonable, and emphasize that the ice phase requires further investigation. Addressing ice particle shape and density variations constitutes an advanced research topic on its own, and we treat it as future work. We hope that this issue will be addressed in our own and other researchers' future studies. We revised the description to this point as following:

Line 237-257

For rain layers, v_t was computed using the empirical relationship proposed in Atlas and Ulbrich (1977), with a correction factor for air density, as given:

$$v_t(D) = -3.78D^{0.67} \cdot c(\rho), \tag{5}$$

$$c(\rho) = \sqrt{\frac{\rho_0}{\rho}} = \sqrt{\frac{\rho_0 RT}{p}}.$$
 (6)

Here, the unit of D is millimeters, ρ denotes the ambient air density, ρ_0 is the standard air density (set to 1.225 kg m⁻³), R is the specific gas constant for dry air (287 J kg⁻¹ K⁻¹), and p and T represent pressure and temperature obtained from auxiliary data. The backscattering cross-section σ_b was derived from Mie scattering calculations for spherical raindrops at W-band frequency.

For snow, σ_b and v_t was calculated in the same manner as in the 2A.DPR algorithm, assuming homogeneous spherical particles with a density of 0.10–0.13 g cm⁻³ and a melted-equivalent diameter following the particle size distribution given by Eq. (3). The terminal fall velocity of snow was calculated following Magono and Nakamura (1965) as follows:

$$v_t(D_s) = -8.8(0.1D_s\rho_s)^{0.5} \cdot c(\rho), \tag{7}$$

where D_s is the unmelted snow particle diameter in mm, and ρ_s is the density of snow particles in g cm⁻³. On the other hand, ice particles can take various shapes, sizes, and densities, such as those of snow, graupel, and hail. Because σ_b and v_t vary depending on these parameters, the assumptions made for snow in this study are often not valid. Although it would be ideal to account for more realistic and complex scattering and fall characteristics of ice particles (Kuo et al. 2016; Ori et al. 2021), considering such diversity is challenging because the CPR observes only in the nadir direction and therefore cannot provide information on particle asymmetry. This contrasts with ground-based dual-polarization radars, which observe the hydrometeor from the side, where particle asymmetry is more evident and can provide additional information. In addition, such information on particle diversity cannot be inferred from the current version of the 2A.DPR algorithm and is therefore left for future work.

6. Figs 2 and 3 are really great:

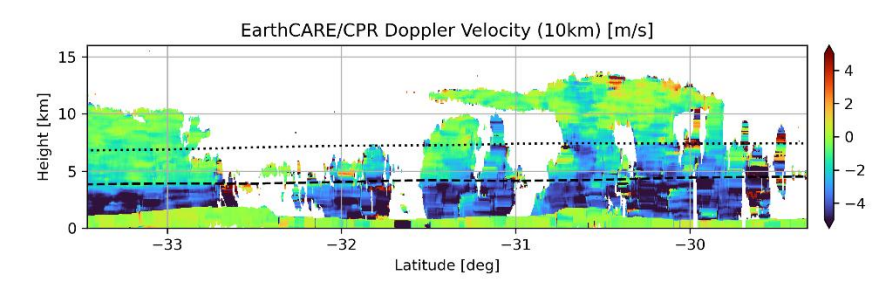
- 1. it's great to see the various Z fields from DPR and ECPR, plus the Doppler!
- 2. The long along-track integration (10 km?) really helps to clean up aliasing in the Doppler and some of the NUBF in Fig.2;
- 3. However, doesn't it also lead to an "over-smoothing" of the Doppler for the convective scene in Fig.3?

Thank you for this valuable comment. First, we would like to clarify that the data included in the coincidence dataset are identical to those in the original EarthCARE/CPR L1b dataset, which provides 500 m horizontally

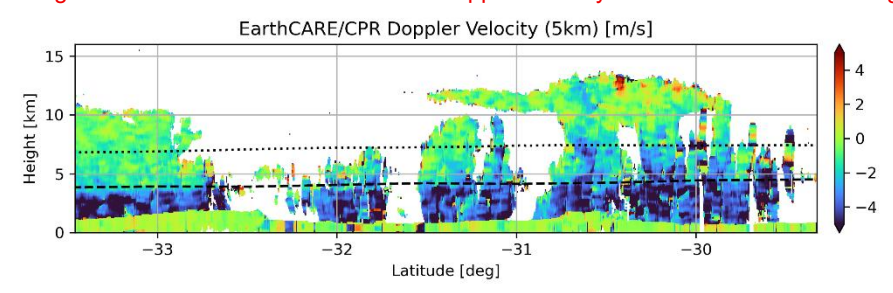
integrated values. The 10 km horizontal integration introduced in this study was an arbitrary length chosen for analytical purposes.

The horizontal 10 km integration is highly effective in reducing the contribution of random noise induced by decorrelation. However, as you pointed out, in convective precipitation this integration may lead to over-smoothing, potentially mixing the signatures of strong echoes within convective cores with weaker echoes at cloud edges.

In response to comments from another reviewer, we have shortened the integration length to 5 km. As a result, the Doppler velocity profiles in Fig. 3d now show reduced horizontal stripe patterns that were present in the original version, while still effectively suppressing random noise and the NUBF effect. This modification alleviated the over-smoothing issue.



Original Fig. 3d. Vertical cross section of CPR Doppler velocity with 10-km horizontal integration.



Updated Fig. 3d. Vertical cross section of CPR Doppler velocity with 5-km horizontal integration.

It should be noted, however, that since the integration is performed as a reflectivity-weighted average rather than a simple moving average, the convective core features tend to be emphasized. This may lead to artificially enhanced downward velocities near cloud edges where echoes are weak. In the statistical analyses presented in Sections 3.2 and 3.3, such edge regions, where the coincidence with DPR observations could not be ensured after averaging, were excluded from the analysis, as indicated by the black-plotted areas in Fig. 3g. Therefore, we believe that the impact of over-smoothing has been effectively mitigated in our results. We have also added the following description:

Line 285-292

The horizontal 5 km integration applied to the V_d field in Fig. 2d is highly effective in reducing the contribution of random noise induced by decorrelation (ε_{random}). However, in the convective case shown in Fig. 3d, this integration may result in over-smoothing, mixing the signatures of strong echoes within convective cores with weaker echoes at cloud edges. Because the integration is performed as a reflectivity-weighted average rather than a simple moving average, the features of the convective core are emphasized, which may in turn lead to artificially enhanced downward velocities near cloud edges where echoes are weak. In the statistical analyses presented later in this paper, such edge

regions, where coincidence with DPR observations could not be ensured after averaging, were excluded from the analysis, as indicated by the black-plotted areas in Figs. 2g and 3g.

7. L.305: Isn't it "CFED of Vd shown in Fig. 4b illustrates an increase in downward velocity with decreasing increasing temperature between -20°C and 0°C,"?

Thank you for pointing this out. The term "decreasing" was incorrect and should be replaced with "increasing."

- 8. The CFEDS of the W band are also great!
 - 1. Fig.4a shows the stagnation of Z around [-10,0]^oC (due to competing effects of increasing unattenuated Z due to growth of particle, and, increasing attenuation) and
 - 2. the slightly increasing Vd in that range shows that there is indeed a growth of particles,

That is exactly the point we have also been focusing on. We believe that the advantage of observing not only Z but also V_d becomes evident in that temperature range. Although this study does not go into that level of detail, we hope that future work involving scattering calculations for snow and ice particles will allow us to relate these observations to temperature-dependent variations in particle shape and density.

- 1. The scatter-plots in Figs 5, 9 and 10 show the various datasets together.
 - 1. Would it help to show the concentration in log(counts) instead of counts? It may be that there aren't enough points to consider a log scale...

We also plotted the color shades in Figs. 5, 9, and 10 on a log scale (Figs. C1, C2, and C3, respectively). The visibility of the figures did not change much compared to the originals. Since plotting in log scale makes it less intuitive to grasp the count values, we prefer to keep the original figures.

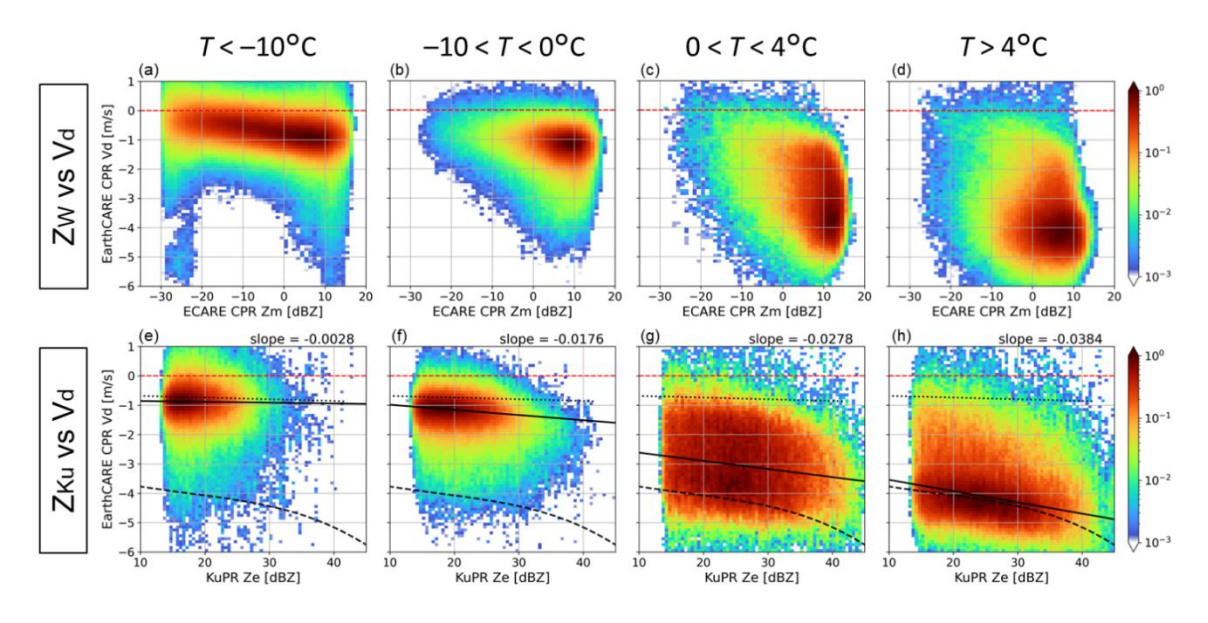


Figure C1: Same as Fig. 5, but with log-scale color shade.

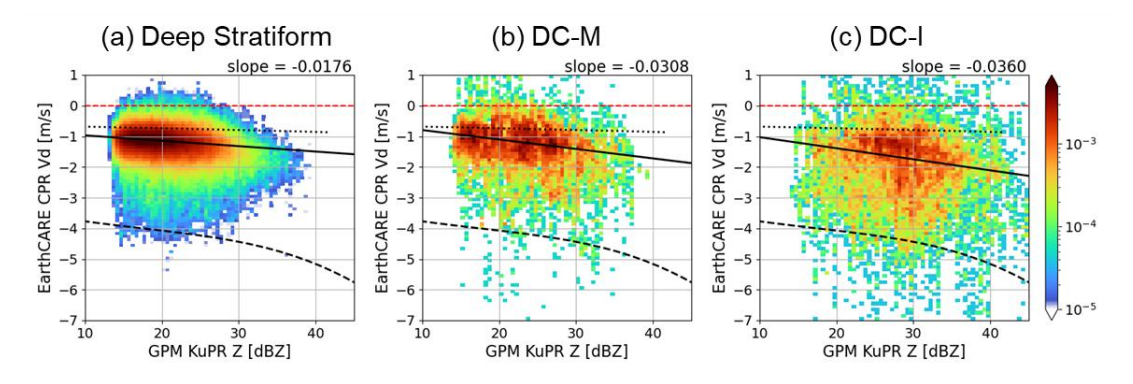


Figure C2: Same as previous Fig. 9, but with log-scale color shade.

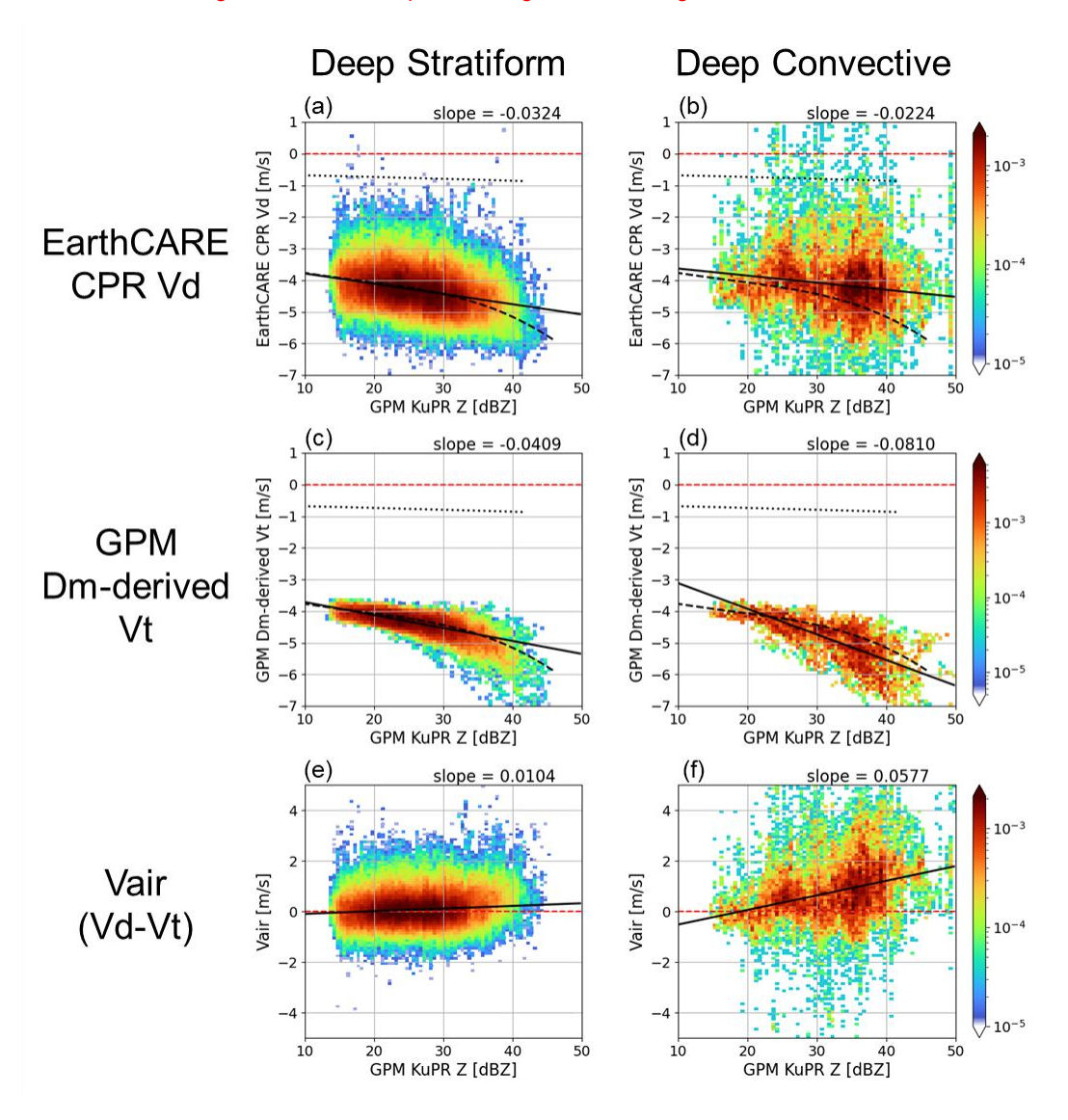


Figure C3: Same as Fig. 10, but with log-scale color shade.

1. L.429 and 501: rimmed or rimed? (please correct various instances in the article).

Thank you. We have revised the manuscript accordingly.

- 2. I was wondering if it would be worth showing plots/statistics of the DWR (ZKu-ZKa) as well?
 - 1. it is directly related to Dm, which plays a central role in the PSD used to estimate Vt in Eqs 3 and 4 and
 - 2. it is a clear indicator when the attenuation of Ka is excessive.

Thank you very much for this important comment. The dual-frequency ratio (DFR or DWR) is indeed theoretically more directly related to the particle size distribution than the reflectivity alone. In response, we have added a diagram in Fig. 9 for the ice phase, using DFR (Z_{Ku}/Z_{Ka}) on the x-axis, and included the following description:

Line 507-520

In some previous studies, the dual-frequency reflectivity ratio (DFR) has been used to characterize ice-phase precipitation (Leinonen et al., 2015; Yin et al. 2017; Akiyama et al. 2025). Compared with using single-frequency Z, DFR cancels the uncertainty associated with the number concentration N_W , thereby is more directly related to the particle size distribution and attenuation. Figures 9d–9f show joint histograms with the Ku–Ka band DFR (Z_{Ku}/Z_{Ka}) from the DPR plotted on the x-axis. Here, we used Z which was not corrected for attenuation. As in the discussion using Z_{Ku} , the convective type tends to show larger DFR values and faster downward V_d compared to the stratiform type, with a steeper regression slope in the DFR- V_d relationship. This suggests the dominance of larger particles with higher density. However, correlation coefficients for each case (Table 1) show that Z_{Ku} correlates more strongly with V_d than DFR does. This simple analysis therefore does not demonstrate a clear advantage of using DFR. The spread of V_d with respect to DFR may reflect the variations in microphysical characteristics such as particle shape and density, as well as atmospheric turbulence. Moreover, because the DFR was calculated using the KaPR HS observation swath, the number of samples is about half that of Figs. 9a–9c, which may have resulted in the lower correlation. As future work, once a larger multi-year dataset becomes available, scattering calculations that account for variations in ice particle shape and density will enable DFR to provide more detailed insights into cloud and precipitation microphysics.

On the other hand, for rain, DFR (Z_{Ku}/Z_{Ka}) tends to take small negative values close to zero around Dm = 0.5–1.5 mm (Fig.1 in Meneghini et al. 2022), which is the range often used as the representative mean raindrop diameter. In this range, the relationship between DFR and particle size becomes ambiguous. While the correlation between DFR and particle size can be improved by using other frequency combinations (e.g., W-and Ka-band), in such cases the strong attenuation and multiple scattering at W-band would need to be carefully addressed. Therefore, the application of DFR in rain remains challenging and is left for future work. We have added the following explanation to the manuscript:

Line 561-566

While a correlation between the DFR and V_d was observed in the ice phase (Fig. 9 and Table 1), in typical rain layers the relationship between raindrop size and DFR becomes ambiguous due to the scattering nature of rain drops (Meneghini et al. 2022). Although using other frequency combinations, such as W- and Ka-band, could improve the correlation between DFR and particle size, interpretation becomes more difficult because of the strong attenuation and multiple-scattering effects at W-band, as shown in Fig. 5d. Therefore, the application of DFR in rain remains challenging and is left for future work.

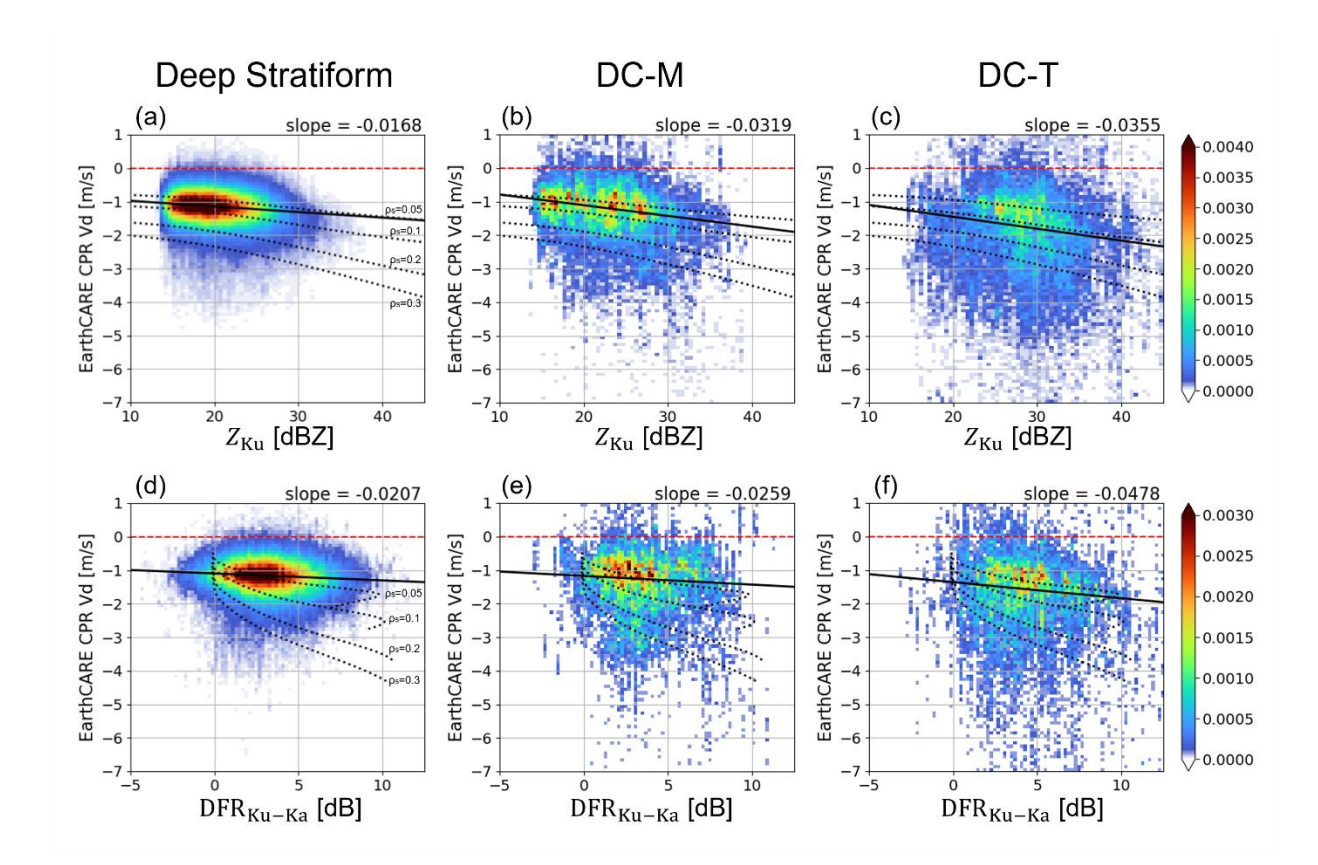


Figure 1: (a–c) Joint histograms of Z_{Ku} and V_d and (d–f) joint histograms of Ku-Ka band dual-frequency reflectivity ratio (DFR) and V_d for temperature range from -10° C to 0° C for (a, d) deep stratiform, (b, e) DC-M, and (c, f) DC-T precipitation types. Each histogram is normalized by the total number of samplings of each precipitation type. The solid black lines represent regression lines fitted using the least squares method, with its corresponding slope indicated in the upper right corner outside each panel. The dotted black lines are same as those in Fig. 5, except that the x-axis is replaced with DFR in (d–f).

Table 1: Correlation coefficients and sample number of the joint histograms of Z_{Ku} – V_d and DFR– V_d for each precipitation type shown in Fig. 9.

Indicator	V _{air} retrieval method	Snow $(-10^{\circ}\text{C} < T < 0^{\circ}\text{C})$		Rain $(T > 4$ °C)	
		a) Stratiform	b) Convective	c) Stratiform	d) Convective
Mean	DPR-based	0.561	0.356	0.279	1.112
	CPR_CLP	0.302	0.621	0.375	1.126
Standard deviation	DPR-based	0.638	1.366	0.874	1.631
	CPR_CLP	0.487	0.945	0.738	1.198

1. In the interpretation of Fig.8, the larger standard deviation of the Doppler is attributed to turbulence. Couldn't it be caused also/instead by 1) shear or 2) the microphysical variability of Vt? Or are these implied in the term "turbulence"?

We agree that shear and microphysical variability are also important factors, and it is better to state this explicitly. We have therefore revised the text as follows:

Line 490-492

Furthermore, the larger standard deviation of V_d compared to that in stratiform precipitation indicates more active turbulent motion, including contributions from vertical air motion, wind shear and microphysical variability.